Evidence for Egg-Box-Compatible Interactions in Calcium-Alginate Gels from Fibre X-ray Diffraction

Pawel Sikorski[1,*], Frode Mo[1], Gudmund Skjåk-Bræk[2], Bjørn T. Stokke[1]

March 6, 2024

[1]Department of Physics, Norwegian University of Science and Technology, Trondheim NO-7491, Norway

[2]Norwegian Biopolymer Laboratory (NOBIPOL), Department of Biotechnology, Norwegian University of Science and Technology, Trondheim NO-7491, Norway

[*]to whom correspondence should be addressed: *pawel.sikorski@phys.ntnu.no*; phone: +4773598393; fax:+4773597710

Abstract

The structure of guluronic acid rich alginate in the acid and calcium forms were investigated using fibre X-ray diffraction. Data recorded for alginate fibres in the acid form show repeat along the chain axis of c= 0.87nm, a value which is in agreement with the one measured by Atkins *et al.* (Biopolymers 1973, 12, 1865) and contradicts repeat of 0.78nm recently suggested by Li *et al.*(Biomacromolecules 2007, 8, 464-468) In the Ca^{2+}-form, our observations indicate that the junction zone involves dimerisation of polymer chains through Ca^{2+} coordination according to the egg-box model. For reasons which are not understood at present, coordination of the divalent cations reduces the ability for the lateral crystallographic packing of the dimers. A proposed model for the junction zone involves polymer chains packed on a hexagonal lattice with lattice constant $a = 0.66$ nm. Random pairs of chains form dimers through coordination of Ca^{2+} cations. Further lateral interaction between dimers is mediated by disordered Na^{+} and Ca^{2+} cations, water molecules and hydrogen bonding.

Introduction

For many ionic polysaccharides, the ability to bind divalent cations and form gels is the key to their biological functions as well as technological applications.[1] Alginic acid (alginate) is a copolymer of β-D-mannuronic acid (M) and α-L-guluronic acid (G). Alginate is a biopolymer mainly isolated from brown algae, and in recent years progress has been made in large scale bacterial synthesis of alginates with desired G and M composition, as well as sequences.[2–4] Alginate belongs to a group of polymers used in the food and pharmaceutical industries as solution property modifiers and gelling agents. Alginates also have a recognised potential in removal of toxic heavy metals from industrial wastes by biosorption.[5] Due to its industrial applications, the alginate gelation process has been studied extensively but still some fundamental questions remain unresolved.

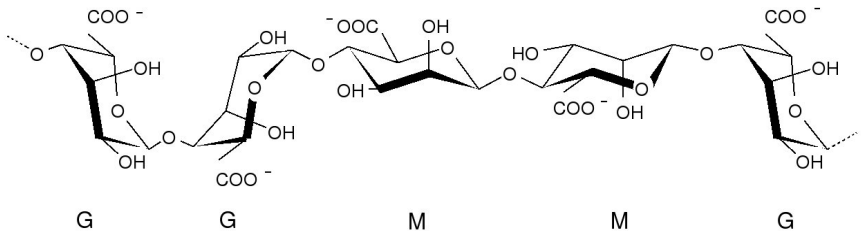

Figure 1: Structure of alginate. β-D-mannuronic acid (M) and α-L-guluronic acid (G). Ring conformation in the alginate chain (M: $^4C_1$ and G: $^1C_4$).[6]

Numerous studies have been performed in order to characterise the mechanisms and structural features involved in the gelation of alginate. Gel formation is linked to specific and strong interactions between long stretches of

G-units and divalent cations like Ca^{2+} or Sr^{2+}. The importance of the G-units in this process is highlighted by the fact that the gel strength is directly related to the total content of G-units and the average length of the G-block in the gelling polymer.[7] Recent studies have also emphasised the importance of the MG repeating units.[8]

Morris *et al.*[9] have shown that Ca^{2+} cations induce interchain association and formation of the gel junction zones. In the generally accepted model, referred to as the egg-box model,[10] divalent cations promote association of pairs of polymer chains (Figure 2a) and the formation of stable junction zones. The schematic egg-box association between G-units, as proposed by Grant *et al.*[10] is shown in Figure 2b. Two pairs of two consecutive G-units, each pair belonging to different polymer chains, are "glued" together through the coordination of a Ca^{2+}-cation. The sugar ring of the guluronic acid is in the $^1C_4$ conformation and the polymer chain adopts a characteristic zig-zag shape. It has been proposed that this shape creates pocket-like cavities in which Ca^{2+}- cations can be easily accommodated. The dialysis experiment showed that a ratio of 4:1 between G-units and Ca^{2+} cations exists in Ca-alginate gels.[9] This fits well with the egg-box model in which specific Ca-mediated interactions involve only 2 polymer chains (see Figure 2) and in the gel state the junction zones do not show a long-range order. The egg-box model has also been used to describe gelling of polygalacturonates (pectins),[11–13] but we restrict our investigation to interaction between G-rich alginate chains.

To date, it has not been possible to verify the egg-box model for interchain

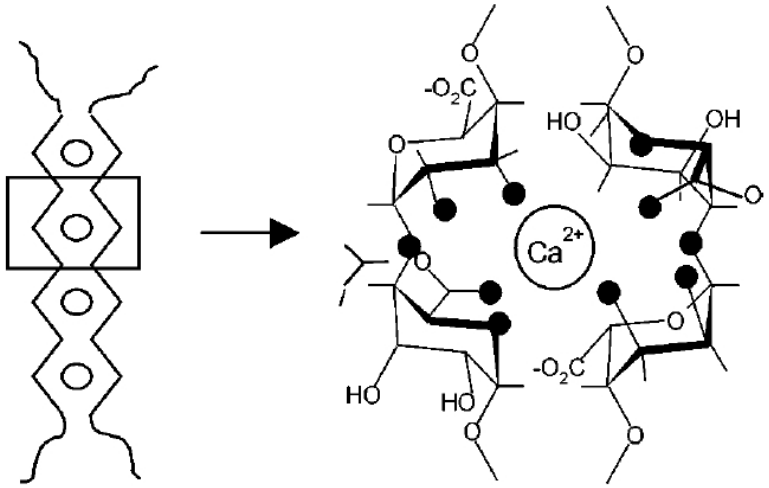

Figure 2: Schematic drawing and calcium coordination of the egg-box model as described for the pair of guluronate chains in calcium alginate junction zones. Dark circles represent the oxygen atoms involved in the coordination of the calcium ion. Reproduced from[12]

association in alginate by any direct structural studies, for example by the fibre X-ray diffraction techniques. To our knowledge, no crystalline and well resolved fibre X-ray diffraction patterns from Ca^{2+}-, Sr^{2+}- (or other divalent cations) forms of G-rich alginate have been published. The only available structural data is for the free acid form.[14] Some diffraction patterns of the low crystallinity Ca^{2+}-form have also been published.[15,16]

The original egg-box model has been reconsidered on a few occasions in recent years. In none of the cases structural data for the Ca^{2+}-form of alginate was used.[12,15–19] Braccini *et al.*[12] conducted molecular modeling studies in which the interaction between pure G-alginate polymer chains and Ca^{2+} cations were optimised. Using the geometry determined for the more crystalline acid form of the polymer chain, a model describing interchain associ-

ation and Ca^{2+} binding was proposed. A different model was proposed by Arnott *et al.*[17] Using the original fibre X-ray diffraction data recorded for the acid form of the G-rich alginate[14] the crystal structures of the acid and the Ca^{2+}-forms were refined. Despite lack of experimental data for the calcium form, a crystal structure and a Ca^{2+} coordination geometry was proposed. In the suggested structure, Ca^{2+} cations replace one of the water molecules found in the unit cell of the free acid form. The chain arrangement and the position of the divalent cations is different from what has been proposed by Braccini *et al.*[12] and is also different from the original features of the egg-box model.[10] Ca^{2+} cations are involved in coordinating 4 polymer chains forming a well organised network of Ca-coordination and hydrogen bonding. This model suggests a long range axial crystalline order within the junction zone.

Small-angle X-ray scattering (SAXS) measurements indicate that in the gel state, the junction zone forms small crystallites incorporating a number of polymer chains. However, SAXS data does not provide any information regarding details of interchain interactions and chain packing but only describes the average size of the junction zones.[18,19] The SAXS data suggested that dimerization of chain segments was the principal association mode at low fractional Ca^{2+} saturation of guluronic acid in the alginate. Increase in the Ca^{2+} concentration resulted in increased lateral association.[18,19]

In the most recent contribution Li *et al.*[16] used fibre and powder X-ray diffraction patterns recorded from low crystallinity alginate samples to draw a number of conclusions about the structure of the junction zone of G-rich alginate in the acid and the Ca^{2+}-forms. We will comment on the

interpretation of the results and compare them with the data presented here.

Experimental Section

Alginate from *L. hyperborea* (stipe) with fraction of G-units $F_G = 0.67$, fraction of two consecutive G-units $F_{GG} = 0.55$, weight average molecular weight $M_w = 400$kDa, and an average length of G-block $N_{G>1} = 14$ was used in all experiments. Fibres were prepared by extrusion of 1% Na alginate solution into a gelling bath. Acid (HCl, pH = 1) and low and high ionic strength calcium gelling baths (Low: 100mM $CaCl_2$, High: 100mM $CaCl_2$ and 200 mM NaCl) were used. Fibres of the length up to 1m could be prepared and a typical gel fibre diameter was $\approx 500\mu m$ (see Figure 3a). After gellation, the fibres were washed in a large amount of deionised H_2O. Some acid fibres were converted into Ca^{2+}-form by soaking in a Ca^{2+}-containing gelling bath. The gel fibres were then stretched using a TA-XT2 Texture Analyser (Stable Micro Systems, Godalming, UK) as they dried slowly in air. The texture analyser allowed stretching under controlled force-extension conditions. A typical stretch ratio obtained was ≈100% and the typical drying/stretching time was 30 min. The final fibre diameter was 30 - 100 μm (see Figure 3b) and the final moisture content was below 5% (measured by determining the change in sample weight on drying in vacuum at 80^oC for 3h).

X-ray diffraction patterns were recorded at the Swiss-Norwegian Beam Lines (SNBL), ESRF, Grenoble, France ($\lambda = 0.87$Å, MAR345 detector) and also using a conventional based generator with a Cu-tube ($\lambda = 1.54$Å, patterns recorded using Fuji image plates (IP) and read with Fuji IP reader).

CCP13 software (www.ccp13.ac.uk) was used for background subtraction.

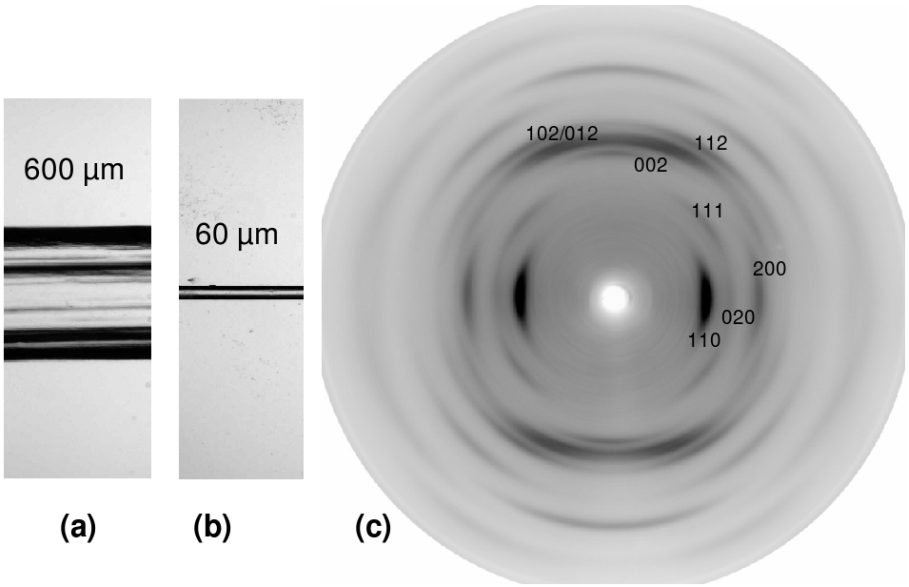

Figure 3: Gel (a) and dried-stretched (b) alginate fibres. (c) fibre X-ray diffraction pattern of G-alginate in the free acid form recorded at SNBL, indices of the main diffraction signals are shown.

Results and Discussion

A fibre X-ray diffraction pattern obtained from G-rich alginate in the acid form with good crystallinity and orientation is shown in Figure 3. Calculated and observed spacings of the main diffraction signals indexed using the unit cell parameters proposed by Atkins *et al.*[14] are listed in Table 1. There is good agreement between the observed and calculated values, confirming that the unit cell is correct.

The diffraction data presented by Li *et al.*[16] have inferior resolution, which resulted in a number of misinterpretations. It was suggested that the repeat

Table 1: Comparison between calculated and observed d_{hkl}, based on the unit cell a=0.86nm, b=1.07nm and c=0.87nm.[14] *s*-strong, *m*-medium, *w*-weak

hkl	d_{cal} [nm]	d_{obs} [nm] ± 0.005 nm	*I* [abs]
110	0.670	0.665	s
020	0.535	0.530	w
200	0.430	0.427	m
111	0.531	0.527	w
002	0.437	0.432	m
012	0.403	0.400	s
102	0.388	0.388	s
112	0.365	0.365	m

along the *c*-axis (chain axis) in the free acid form of G-alginate is close to 0.78nm, compared to a value of 0.87nm determined earlier.[14] For samples with poor crystallinity and orientation as those published by Li *et al*,[16] the 002 reflection is very weak (compare patterns in Figure 3 with a lower crystallinity pattern shown in Figure 5a), and two strong signals at 0.403nm and 0.388nm (012 and 102) merge to form a strong broad signal located at around 0.39nm. This is clearly visible in Figure 4, where diffraction data have been integrated and presented in a form of powder diffraction pattern. The 0.39nm signal was mis indexed by Li *et al.*[16] as 002, where in fact in the powder pattern the 002 signal is masked by the equatorial 200 signal (Figure 4). As the diffraction data presented here and data published by Li *et al*[16] show the same main features we can argue that possible variations in the chemical composition of the alginate used in the two studies affect our conclusions (both polymer have similar total G-content).

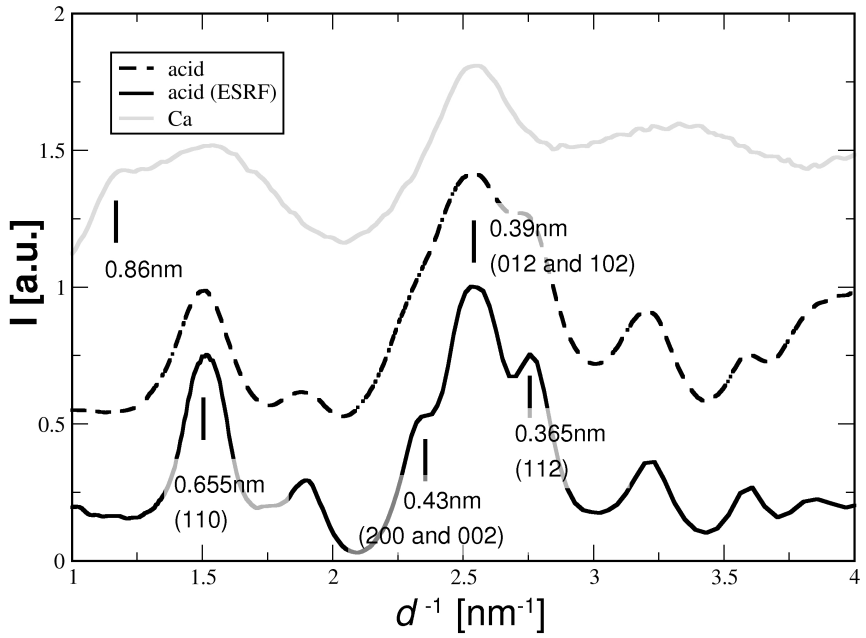

Figure 4: Fibre X-ray diffraction patterns for acid and Ca^{2+}-forms of G-rich alginate which have been integrated and presented in a form of powder diffraction patterns. For the acid form, the 002 diffraction signal is not easily observed as it overlaps with the 200 signal

More crucially Li *et al.*[16] use low resolution diffraction data to suggest that in the Ca^{2+}-form the G-rich alginate chain has a 3_1 helical conformation. This is in contrast to the 2_1 conformation observed in the acid form. We do not agree with this interpretation of the diffraction results and present data which supports a 2_1 conformation and the packing of the polymer chains within the junction zone compatible with the egg-box model.

Regardless of preparation and annealing procedures, we have not been able to prepare well diffracting crystalline samples of the Ca^{2+}-form of G-rich alginate. It is possible to prepare samples with good orientational order of the polymer chains (*i.e.* nematic order), but the crystallinity is always

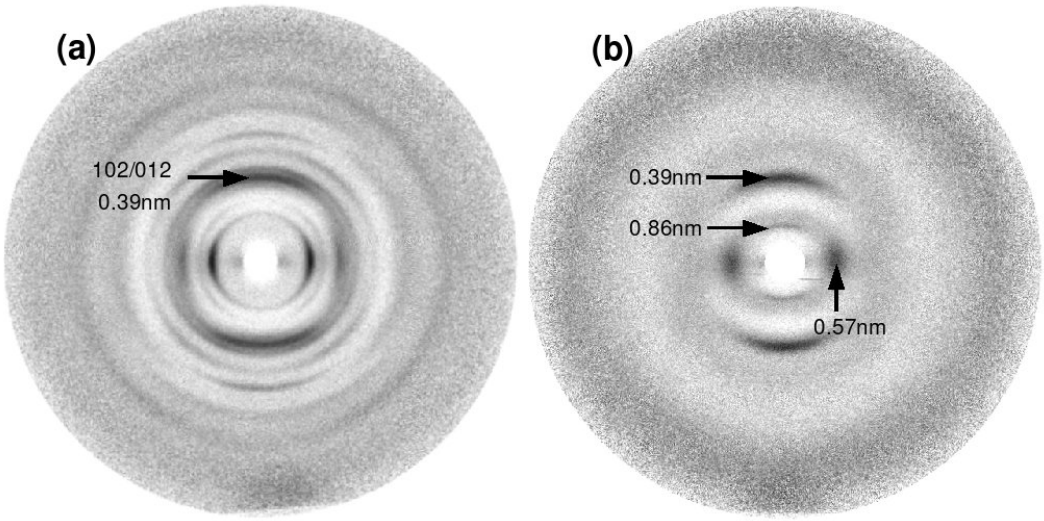

Figure 5: Fibre X-ray diffraction recorded for (a) H^+-form gel fibre stretched by 100% and annealed for 24h 100 ^{o}C at high RH and (b) Ca^{2+}-gel fibre stretched 75%, annealed for 24h 100 ^{o}C at high RH, prepared at high ionic strength conditions. Both patterns were recorded using a Cu-tube X-ray source ($\lambda = 1.54$Å).

low. The diffraction patterns observed for the Ca^{2+}-form of G-rich alginate are very similar regardless of the sample preparation method. This includes gel fibres made by extruding alginate solution directly into a Ca^{2+}-containing solution (100mM $CaCl_2$), fibres converted from acid to the Ca^{2+}-form, or the sample prepared by starting from a Na-alginate film which is then soaked in a Ca^{2+}-containing solution. It is known that the acid form is crystalline, and it is possible to convert it into the Ca^{2+}-form by soaking in a $CaCl_2$ solution (100 mM). Using this procedure, again only low crystallinity patterns similar to that shown in Figure 5b could be obtained. At the same time the orientation of the polymer chains within the sample was maintained (as indicated by orientation order observed in the diffraction patterns). Surprisingly, on

Table 2: Diffraction signals observed for Ca^{2+}-form of G-rich alginate, *s*-strong, *m*-medium, *w*-weak

d_{obs} [nm] ± 0.01 nm		I
0.57	*broad*	*s*
0.86	*sharp*	*m*
0.39	*broad*	*s*

conversion back into the acid form (by soaking in a HCl solution, pH=1), crystallinity was regained. These observations suggest that packing of the polymer chains in the Ca^{2+}-form must be different from the acid form and there must be some inherent structural reason for the change in crystallinity.

A fibre X-ray diffraction pattern recorded for G-rich alginate in the Ca^{2+}-form is shown in Figure 5b. Three main signals are observed: a broad and strong equatorial diffraction signal at 0.57nm; a sharp, meridional or close to meridional signal at 0.86nm and a strong meridional or off-meridional at 0.39nm (see Table 2).

The meridional signal at 0.86nm is especially interesting. The observed spacing is close to that predicted for the 001 reflection of the acid form ($d_{001} = 0.87nm$). However in the acid form this reflection is systematically absent due to the 2_1 chain conformation. For a polymer chain in the 2_1 conformation, intensity close to the meridian on the first layer line is not expected even for a sample with poor crystallinity (see below). This signal is missing on a pattern recorded for stretched films of Na G-rich alginate (data not shown), a pattern which otherwise is similar to the one shown in Figure

5b.

We hypothesize that the distribution of Ca^{2+} cations within the junction zone contributes to the intensity observed close to the meridian on the first layer line. The distribution of strongly scattering Ca^{2+} cations along the chain axis at a repeat distance of 0.86 nm would break the 2_1 symmetry. Interestingly, Ca^{2+} cations separated by a distance of 0.87 nm along the chain axis are predicted by an egg-box like interaction between alginate chains (four sugar units from two polymer chains coordinating a single Ca^{2+} cation)

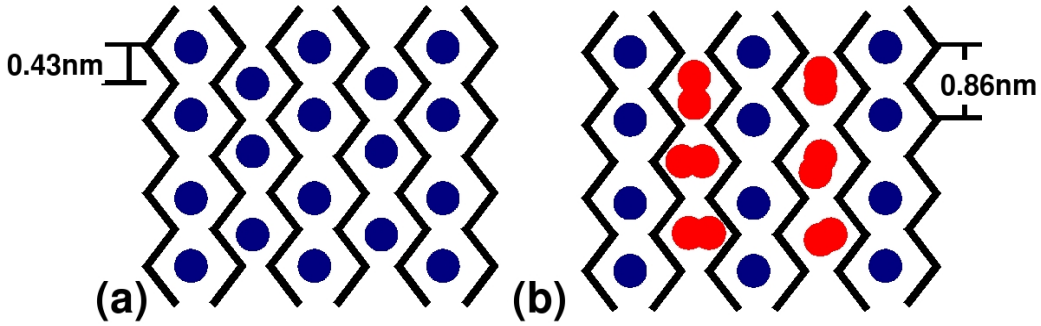

Figure 6: Schematic structure of G-alginate junction zone. (a) long range Ca^{2+}-mediated interaction between chains (b) Ca^{2+}-mediated dimers which pack through unspecific interactions. The diffraction data points to situation *b*.

The intensity of the 001 diffraction signal is affected by the lateral order within the junction zone. Long range order between dimers as shown schematically in Figure 6a would require Ca^{2+} cations to be located at two defined crystallographic positions (axial translation with respect to each other by $c/2$= 0.43nm). This introduces additional symmetry to the structure (now also Ca^{2+} cations follow the 2_1 symmetry), and the 001 signal should be systematically absent. Non-zero intensity of the 001 diffraction signal

indicates that the association of dimers take place through unspecific interactions, like water mediated hydrogen bonding and disordered Ca^{2+}- and Na^{+} cations (Figure 6b).

3_1 versus 2_1 conformation

Before proposing a model for the junction zone, let us consider carefully the conformation of the alginate chain and investigate the diffraction pattern expected for a 3_1 helical conformation as suggested by Li *et al.*[16] The diffraction from helical molecules has been studied extensively in the past.[20–22] A diffraction pattern for a single polymer chain in a helical conformation is described by the cylindrically average intensity transform of the discontinuous helix:[22]

$$\langle I(R, l/c)\rangle_{\psi} = \sum_{n} J_n^2 \left(2\pi R r\right) \tag{1}$$

where l is the layer line index, c is the repeat along the chain axis, J_n denotes an nth-order Bessel function, r is the helix radius and R is the reciprocal space coordinate in the equatorial direction. The summation extents over all n-values that satisfy eq. 2.

$$l = um + vn \tag{2}$$

where u is the number of units in v turns ($u = 3$ and $v = 1$ for a 3_1 helix).

For a 3_1 helix the diffraction pattern will contain layer lines spaced at c^{-1} . Diffracted intensities on the layer lines with $l = 0, 3, 6, ...$ are proportional to $J_0^2 + J_3^2 + ...$ and for $l = 1, 2, 4, 5, 7, 8, ...$ are proportional to $J_1^2 + J_4^2 + ...$ Schematic diffraction patterns calculated for a polymer chain in 2_1, 3_1 and

4_1 conformations using the CCP13 program HELIX[23] are shown in Figure 7. As expected from eq.1, intensity close to the meridian is observed only on the 3rd, 6th etc layer lines for a 3_1 helix, and it is zero on all other layer lines (Figure 7b). The described situation will not change significantly for a case where helices are arranged on a crystalline lattice. Instead of a continuous intensity, crystalline order will sample the intensity on the layer lines, and discrete spots will appear instead of continuous streaks. The intensity of the individual spots will still be proportional to what is seen for a single helix.

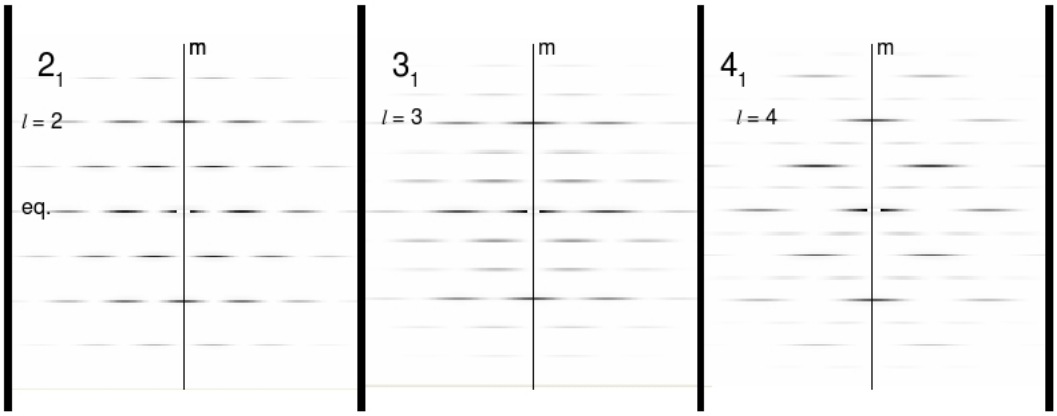

Figure 7: Schematic diffraction patterns calculated using program HELIX[23] (www.ccp13.ac.uk) for polymer chains in a 2_1, 3_1 and 4_1 helical conformations. Repeat along the c-axis are $2c_0$, $3c_0$ and $4c_0$, were c_0 is raise per monomer unit. Note that meridional reflections are observed at the layer line with the same reciprocal coordinate corresponding to c_0^{-1}. *eq.* - equator, m - meridian.

In the acid form, the G-alginate is in a 2_1-conformation, with a c-repeat of 0.87nm. The advance per single G-unit is 0.435nm. If the chain was to be "twisted" into a 3_1-conformation, the advance per monomer would most likely change by some small amount. Pectic acid, which is similar to guluronic acid, contains two equatorial linkages and exists in a 3_1 conformation.[13] For

this polymer the axial advance per monomer is 0.445nm.[13] In addition there is only a small change in the repeat distance between 3_1 and 2_1 conformations as shown by molecular modeling studies.[12] Therefore, we can assume that the advance per G-unit for a hypothetical alginate chain in a 3_1 conformation would be between 0.40 and 0.45 nm. For a 3_1-conformation, the repeat along the chain axis would contain three monomers, and as a consequence the *c*-repeat would be between 1.20nm and 1.35nm. Therefore, for a 3_1 conformation, layer lines at reciprocal coordinates $(1.275 \pm .075nm)^{-1}$, $(0.638 \pm 0.038nm)^{-1}$ and $(0.425 \pm 0.025nm)^{-1}$ are expected. This is clearly not the case for patterns observed for the Ca^{2+}-form of G-rich alginate presented here and those published by Li et al.[16] As a consequence, the 3_1 conformation for Ca^{2+}-form of the G-rich alginate can be ruled out.

As described above, the presence of meridional intensity on the first layer line (located at $(0.86nm)^{-1}$) can not be interpreted as an indication of a 3_1 helix, but rather points to a chain in a 2_1 conformation with its symmetry broken by Ca^{2+} cations spaced by 0.86 nm.

Chain packing

Data on the diffraction pattern allows us to construct a simple model for the Ca^{2+}-alginate junction zone. We have to keep in mind that due to low information content of the diffraction pattern, this is not a definite model, but it represents one way to pack polymer chains which is consistent with the observed diffraction pattern.

Diffraction intensities observed on the first layer line are consistent with

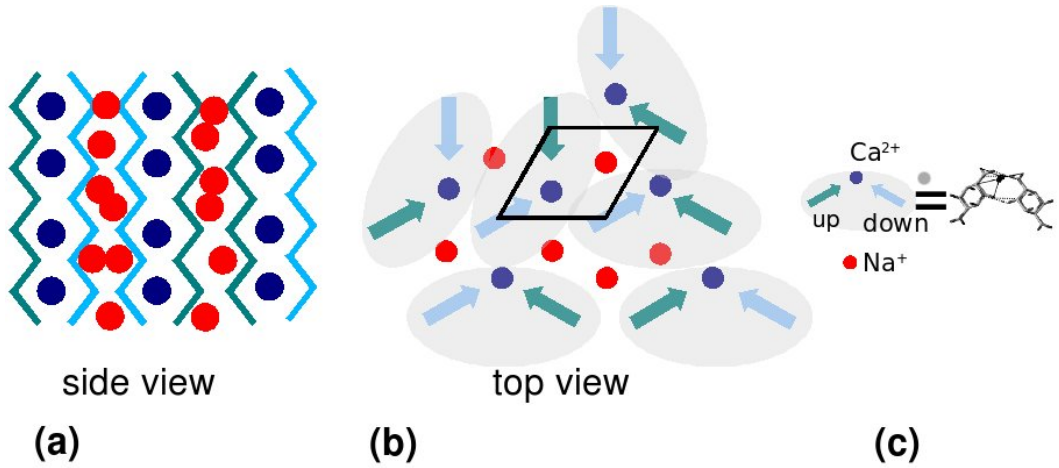

Figure 8: Hypothesised model for the chain packing within a G-rich alginate junction zone in agreement with the diffraction data. In (b) alginate chains are represented by arrows, green for chain up and blue for chain down; arrows are pointing towards Ca^{2+} cations (dark blue) coordinated by a given chain. Na^{+} cations are shown in red; There are only two chains per column of Ca^{2+} cations and egg-box like dimers are indicated by light grey ellipses; (c) packing of chains in a egg-box like dimer based on molecular simulations. Part of (c) reproduced from.[12] The average distance between polymer chains is 0.66nm, but it is possible that this distance varies between Ca^{2+}- and Na^{+}-mediated interactions. This difference is however not resolved by the diffraction data and the figure represents an average distance.

the basic scattering unit composed of two polymer chains in a 2_1 conformation coordinating one Ca^{2+} cations for every 4 G-units (2 in each chain). One way in which those dimers can then pack to form larger junction zones is on a hexagonal lattice, as shown in Figure 8.[24] Figure 8b shows a view parallel to the polymer chain axis. Grey shaded ellipses represent two polymer chains which coordinate Ca^{2+} cations shown in blue (egg-box like dimer). The polymer chains are centred on a hexagonal lattice. The lattice spacing can be calculated from the observed 0.57nm diffraction signal, assuming that this is the first strong signal for a hexagonal lattice (100). The calculated

lattice spacing which represents the average distance between the centres of the polymer chains is $a = 0.66$nm. This value is sterochemically feasible and similar to what has been found in molecular modeling simulations.[12]

Conclusions

Fibre X-ray diffraction data recorded for G-rich alginate fibres in the acid form show repeat along the chain axis of c= 0.87nm in agreement with the model by Atkins *et al.*[14] In the Ca^{2+}-form, our observations indicate that the junction zone involves dimerisation of polymer chains through Ca^{2+} coordination according to the egg-box model. For reasons which are not understood at present, coordination of the Ca^{2+} cations reduces the ability for lateral packing (smectic order) of the dimers. Hence, the reversible interconversion between acid and salt forms involves a shift in the balance between smectic (crystalline) and nematic (not crystalline) order which is clearly demonstrated by the fibre X-ray diffraction patterns. The proposed model for the junction zone involves polymer chain packed on a hexagonal lattice with the lattice constant $a = 0.66$ nm. Random pairs of chains form dimers through coordination of Ca^{2+} cations. Further lateral interaction between dimers is mediated by disordered Na^{+} and Ca^{2+} cations, water molecules and hydrogen bonding.

Acknowledgements

P.S. acknowledges financial support from The Norwegian Research Council under Centre for Biopolymer Engineering at NOBIPOL, NTNU (Grant No. 145945/130) and SNBL staff for help with the diffraction experiments (EXPERIMENT 01-02-649).

References

1. Moe, S.; Draget, K. I.; Skjåk-Bræk, G.; Smidsrød, O. In Food Polysaccharides and Their Applications. In ; Stephen, A., Ed.; Marcel Dekker: New York, 1995.

2. Valla, S.; SkjakBraek, G. *Agro. Food Industry Hi-Tech* **1996,** *7,* 38 – 41.

3. Rehm, B. H. A.; Valla, S. *Applied Microbiology and Biotechnology* **1997,** *48,* 281 – 288.

4. Ertesvag, H.; Valla, S. *Polymer Degradation and Stability* **1998,** *59,* 85 – 91.

5. Davis, T. A.; Volesky, B.; Mucci, A. *Water Research* **2003,** *37,* 4311 – 4330.

6. Smidsrod, O.; Glover, R. M.; Whittington, S. *Carbohydrate Research* **1973,** *27,* 107 – 118.

7. Draget, K. I.; SkjakBraek, G.; Smidsrod, O. *International Journal of Biological Macromolecules* **1997,** *21,* 47 – 55.

8. Donati, I.; Holtan, S.; Morch, Y. A.; Borgogna, M.; Dentini, M.; Skjak-Braek, G. *Biomacromolecules* **2005,** *6,* 1031 – 1040.

9. Morris, E. R.; Rees, D. A.; Thom, D.; Boyd, J. *Carbohydr. Res.* **1978,** *66,* 145 – 154.

10. Grant, G. T.; Morris, E. R.; Rees, D. A.; Smith, P. J. C.; Thom, D. *FEBS Lett.* **1973,** *32,* 195 – 198.

11. Ravanat, G.; Rinaudo, M. *Biopolymers* **1980,** *19,* 2209 – 2222.

12. Braccini, I.; Perez, S. *Biomacromolecules* **2001,** *2,* 1089 – 1096.

13. Walkinshaw, M. D.; Arnott, S. *J. Molec. Biol.* **1981,** *153,* 1055 – 1073.

14. Atkins, E.; Nieduszynski, I.; Mackie, W.; Parker, K.; Smolko, E. *Biopolymers* **1973,** *12,* 1865.

15. Mackie, W.; Perez, S.; Rizzo, R.; Taravel, F.; Vignon, M. *Int. J. Biol. Macromol.* **1983,** *5,* 329 – 341.

16. Li, L.; Fang, Y.; Vreeker, R.; Appelqvist, I.; Mendes, E. *Biomacromolecules* **2007,** *8,* 464–468.

17. Arnott, S.; Bian, W.; Chandrasekaran, R.; Manis, B. *Fibre Diff. Rev.* **2000,** *36,* 44.

18. Stokke, B. T.; Draget, K. I.; Yuguchi, Y.; Urakawa, H.; Kajiwara, K. *Macromol. Symp.* **1997,** *120,* 91 – 101.

19. Stokke, B. T.; Draget, K. I.; Smidsrod, O.; Yuguchi, Y.; Urakawa, H.; Kajiwara, K. *Macromolecules* **2000,** *33,* 1853 – 1863.

20. Cochran, W.; Crick, F. H. C.; Vand, V. *Acta Crystallographica* **1952,** *5,* 581 – 586.

21. Franklin, R. E.; Klug, A. *Acta Crystallographica* **1955,** *8,* 777 – 780.

22. Fraser, R.; MacRae, T. *Conformation in Fibrous Proteins and Related Synthetic Polypeptides;* Academic Press: New York, 1973.

23. Knupp, C.; Squire, J. M. *J. Appl. Crystallogr.* **2004,** *37,* 832 – 835.

24. By hexagonal arrangement we do not mean a true hexagonal symmetry in a crystallographic sense. We envisage polymer chains that are located on lattice point of a hexagonal lattice with a = 0.66nm. Chain setting angle (rotation along the chain axis) and the position of the complexing ions does not follow the hexagonal symmetry.

Table of Contents Graphic